Functional and structural insights into a novel promiscuous ketoreductase of the lugdunomycin biosynthetic pathway

Xiao, X.; Elsayed, S.S.M.A.; Wu, C.; Heul, H.U. van der; Metsä-Ketelä, M.; Du, C.; ... ; Wezel, G.P. van

ACS chemical biology

pubs.acs.org/acschemicalbiology

Articles

Functional and Structural Insights into a Novel Promiscuous Ketoreductase of the Lugdunomycin Biosynthetic Pathway

Xiansha Xiao, Somayah S. Elsayed, Changsheng Wu, Helga U. van der Heul, Mikko Metsä-Ketelä, Chao Du, Andrea E. Prota, Chun-Chi Chen, Weidong Liu, Rey-Ting Guo, Jan Pieter Abrahams, and Gilles P. van Wezel*

Cite This: *ACS Chem. Biol.* 2020, 15, 2529−2538

Read Online

ACCESS | Metrics & More | Article Recommendations | Supporting Information

ABSTRACT: Angucyclines are a structurally diverse class of actinobacterial natural products defined by their varied polycyclic ring systems, which display a wide range of biological activities. We recently discovered lugdunomycin (**1**), a highly rearranged polyketide antibiotic derived from the angucycline backbone that is synthesized via several yet unexplained enzymatic reactions. Here, we show via *in vivo*, *in vitro*, and structural analysis that the promiscuous reductase LugOII catalyzes both a C6 and an unprecedented C1 ketoreduction. This then sets the stage for the subsequent C-ring cleavage that is key to the rearranged scaffolds of **1**. The 1.1 Å structures of LugOII in complex with either ligand 8-*O*-Methylrabelomycin (**4**) or 8-*O*-Methyltetrangomycin (**5**) and of apoenzyme were resolved, which revealed a canonical Rossman fold and a remarkable conformational change during substrate capture and release. Mutational analysis uncovered key residues for substrate access, position, and catalysis as well as specific determinants that control its dual functionality. The insights obtained in this work hold promise for the discovery and engineering of other promiscuous reductases that may be harnessed for the generation of novel biocatalysts for chemoenzymatic applications.

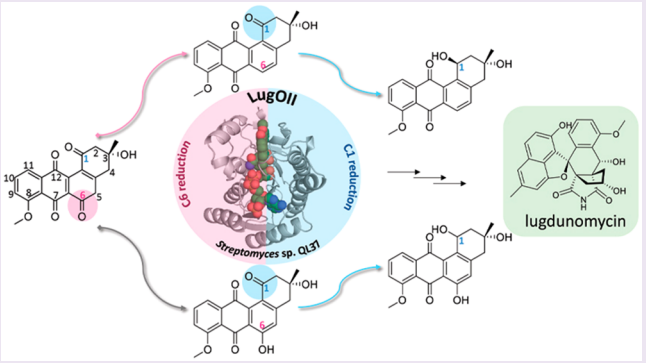

INTRODUCTION

Angucyclines represent by far the largest group of polycyclic aromatic polyketides, which are rich in structural features, and show diverse biological profiles, predominantly anticancer and antibacterial.[1] As exemplified by the promising angucycline drugs landomycin,[2] urdamycin,[3] jadomycin,[4] and gilvocarcin,[5] angucyclines have been attractive targets for synthetic organic chemistry as well as for biological activity studies. Investigations into their biosynthesis led to the discovery of novel angucyclines, including new catalytic mechanisms and enzymology.[6,7] The Gram-positive *Actinobacteria* are a major source of bioactive natural products, the majority of which are produced by members of the genus *Streptomyces*.[8,9] Despite the increasing difficulty to isolate novel bioactive metabolites, *Streptomycetes* still have a huge biosynthetic potential.[10,11] This is due to the fact that many of the biosynthetic gene clusters (BGCs) are poorly expressed in the laboratory, generally referred to as silent or cryptic BGCs.[12,13] One such cryptic BGC is that for the antibiotic lugdunomycin (**1**), an angucycline-derived polyketide produced by *Streptomyces* sp. QL37. Lugdunomycin has antibiotic activity against Gram-positive bacteria, with an MIC of around 25 μg mL^{-1} against *Bacillus subtilis*.[14] The molecule has an unprecedented complex skeleton, composed of a heptacyclic ring, a spiroatom, a benzaza[4,3,3]propellane moiety, and two all-carbon stereocenters.[14] The backbone of **1** is generated from acetate and malonate subunits by the iterative action of a type II polyketide synthase (PKS). The early biosynthetic steps yield the core structure UWM6 (**2**) or prejadomycin (**3**), which undergoes early stage tailoring reactions and is converted to 8-*O*-methylrabelomycin (**4**) and then 8-*O*-methyltetrangomycin (**5**) and tetrangulol methyl ether (**6**), which then serve as the key intermediates for the subsequent Baeyer−Villiger oxidation at the C6a−C7 bond of ring C (Scheme S1). Structural rearrangement and the introduction of a nitrogen atom afford limamycins, which react in a cascade of oxidative C−C bond cleavage and aldol condensation, leading to the production of iso-maleimycin.[15] Finally, the Diels−Alder [4 + 2] cycloaddition step between iso-maleimycin and the hydroxy-*o*-quinodimethane intermediate resulted in the generation of **1**. In addition to **1**, 11 newly rearranged and nonrearranged

Received: July 10, 2020
Accepted: August 25, 2020
Published: August 25, 2020

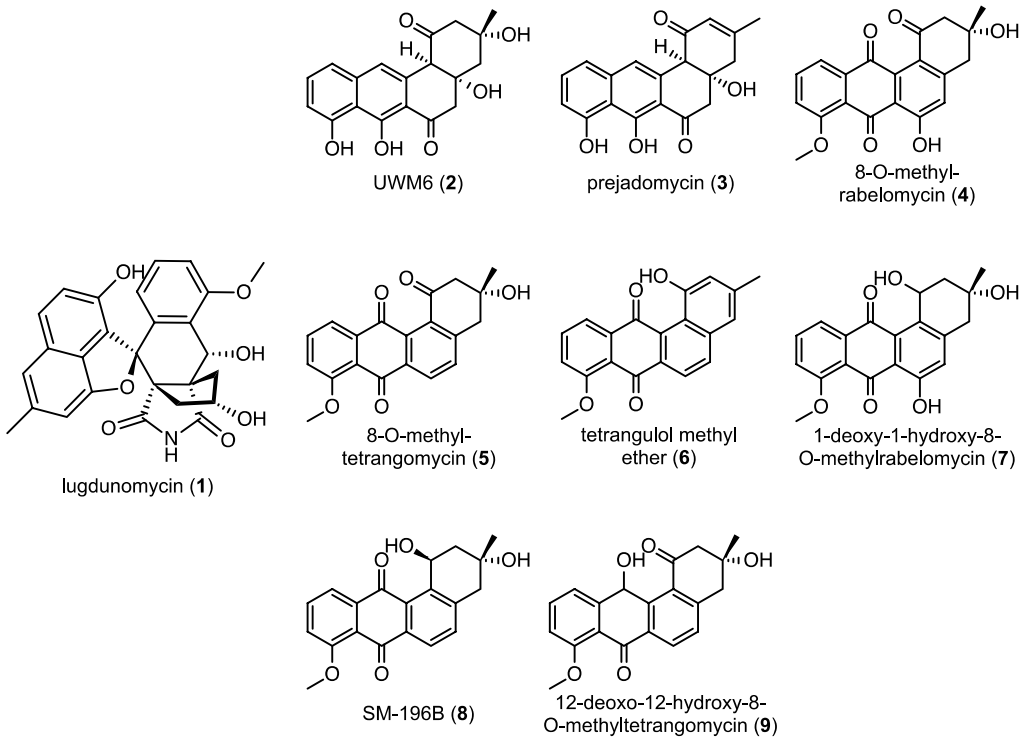

Figure 1. Structures of the metabolites discussed in this study. Lugdunomycin (**1**), UWM6 (**2**), prejadomycin (**3**), 8-*O*-methylrabelomycin (**4**), 8-*O*-methyltetrangomycin (**5**), tetrangulol methyl ether (**6**), 1-deoxo-1-hydroxy-8-*O*-methylrabelomycin (**7**), SM-196B (**8**), and 12-deoxo-12-hydroxy-8-*O*-methyltetrangomycin (**9**).

angucyclines featuring diverse patterns were discovered. In light of the intriguing ring cleavages, aldol condensation, and Diels−Alder cycloaddition, the *lug* gene cluster presents a unique opportunity to study the versatile post-PKS tailoring reactions.

The *lug* gene cluster (Figure S1) encodes a minimal PKS complex, regulators, transporters, and a series of post-PKS tailoring enzymes, including oxygenases, reductases and group transferases. The role of the minimal PKS in the production of the angucycline backbone has been well studied in many families of the angucycline antibiotics.[1,7] However, understanding the enzymology behind the chemical transformations is needed to expand our knowledge of lugdunomycin (**1**) biosynthesis. Reductases, as one of the most powerful synthetic chemical transformants, have been employed by introducing complex chiral centers in natural products. The archetypal example is ActKR, a regio- and stereospecific C9 ketoreductase in the synthesis of the antibiotic actinorhodin, in which single mutations could convert stereospecificity to either an *R*- or *S*-dominant product.[16] Another widely studied example is LanV, which carries out a C6 ketoreduction during the biosynthesis of landomycins, a promising group of anticancer agents.[17,18] The stereochemical outcomes of LanV are controlled more by the conformational changes of the substrate, rather than by the enzyme itself.[17,18] Structural studies of the ketoreductases revealed typical Rossman folds that are shared by the short-chain alcohol dehydrogenase/reductase (SDR) family of enzymes.[16,19] Investigations into the active site architecture highlighted differences in substrate specificity and the stereochemical outcome of the ketoreduction of LanV compared to UrdMred, PgaMred, and CabV.[17,18]

Herein, we describe the identification and characterization of LugOII as a promiscuous ketoreductase that plays a key role in lugdunomycin (**1**) biosynthesis. We determined the crystal structure of LugOII bound to its substrates and, specifically, revealed the structural changes in the enzyme during catalysis. Mutational analysis of the active site provided details on unique features contributing to its dual functionality. These data expand our understanding of LugOII in generating a great diversity of angucycline analogs.

RESULTS AND DISCUSSION

Identification of LugOII, an Atypical Reductase in the Lugdunomycin Pathway. We explored the enzymatic basis for the observed chemical transformations leading to the production of lugdunomycin (**1**) (Figure 1). The *lug* gene cluster encodes polyketide synthases and putative oxygenases and reductases (Figure S1). A comparison of the *lug* gene cluster with the related gene clusters *pga* (gaudimycin), *urd* (urdamycin), *lan* (landomycin), and *jad* (jadomycin) revealed that *lugA-lugF* are the minimal PKS genes required for the biosynthesis of **2**, the first stable angucycline intermediate[14] (Scheme S1). Subsequent spontaneous dehydration should then result in **3**. *LugM* encodes a methyltransferase, which is likely to be involved in the methylation of **2** and/or **3**.[14] A C12 hydroxylation then takes place in the next step by the FAD-binding oxygenase LugOI, which is a homologue of PgaE, UrdE,[20] and LanE.[21] Additionally, we identified LugOII, which consists of two domains, an N-terminal FAD-binding flavoprotein domain and a C-terminal SDR domain. The enzyme shares over 60% amino acid identity with UrdM, PgaM, LanM2,[22] and BexM,[23] which are encoded by the BGCs of urdamycin, gaudimycin, landomycin, and BE-7585A, respectively (Figures S3 and S4). The reductase domains of UrdM and PgaM[21,24] catalyze a C6 ketoreduction. The high similarity between the reductase domains of LugOII, UrdM,

https://dx.doi.org/10.1021/acschembio.0c00564
ACS Chem. Biol. 2020, 15, 2529−2538

and PgaM suggests that LugOII may carry out a reduction at C6 after the action of LugOI. Thus, we set out to study the function of LugOII in lugdunomycin biosynthesis.

Besides a start codon at the beginning of the gene, *lugOII* also possesses an internal start codon at about two-thirds of the gene, suggesting a nested gene system, which was observed in its homologue *pgaM*.[25] To investigate the complex formation of LugOII *in vivo*, we placed the entire *lugOII* gene under the control of the constitutive and strong *ermE** promoter in a *lugOII* null mutant of *Streptomyces* sp. QL37. This indeed resulted in the production of two protein forms that corresponded in size to the 70 kDa full-length LugOII and the 27 kDa LugOII reductase domain (Figure S2). Both fragments were verified by liquid chromatography coupled to mass spectrometry (LC-MS/MS).

LugOII Acts as a C6 Reductase during Lugdunomycin Biosynthesis. To investigate the biosynthetic role of LugOII, we constructed a *lugOII* null mutant (see Methods for details). *Streptomyces* sp. QL37 and its *lugOII* null mutant were grown on both R5 and on minimal media (MM) agar plates for 7 days, after which the agar was extracted with ethyl acetate followed by LC-MS. **1** was only produced by the wild-type strain on MM. Analysis of the LC-MS data revealed that on R5 agar the production of **5** and **6** (Figure 1) was abolished in Δ*lugOII*, indicating an essential role of the enzyme in the angucycline biosynthetic pathway (Data S1). The production of **5** and **6** was restored in a complemented mutant that expresses *lugOII* from the constitutive *ermE** promoter. Additionally, a peak corresponding to the previously described 12-deoxo-12-hydroxy-8-*O*-methyltetrangomycin (**9**)[14] was absent in the metabolic extracts of Δ*lugOII* (Data S1A,B). The production of the molecule was also restored in the complemented mutant grown on R5. The absence of **5**, **6**, and **9** in the deletion strain and their restoration in the genetically complemented mutant expressing *lugOII* suggest that LugOII may bear C6 reduction activity, which is consistent with its similarity to enzymes carrying out similar reactions. Notably, on MM, the production of **1** was abolished in the deletion mutant, indicating that *lugOII* likely ensures the production of precursors that are essential for its biosynthesis (Data S1B). Colonies of the complemented mutant did not grow well on MM, and the production of **1** in this strain was therefore not evaluated. Conversely, the biosynthesis of **4**, which bears an oxidized C6, was not affected in *lugOII* mutants grown on R5 or MM agar. On the basis of similar metabolites observed in the biosynthetic pathways of gilvocarcin and fluostatin angucyclines,[26,27] the desmethyl derivative of **4** (rabelomycin) can be a spontaneous product of **2** and/or **3**, the key intermediates in angucycline biosynthesis.[28,29]

***In Vitro* Characterization Confirms That LugOII Is a Promiscuous Reductase That Also Carries out C1 Reduction.** To further explore the catalytic nature of LugOII, compounds **4** and **5** were selected for an *in vitro* reaction with the enzyme. Recombinant LugOII was purified to homogeneity, and enzymatic reactions were performed, followed by extraction with ethyl acetate for LC-MS analysis. Incubation of **4** with LugOII resulted in the consumption of the substrate and the appearance of **7** (Figure 2a,b). Meanwhile, the enzymatic reaction of **5** with LugOII resulted in the production of **8** (Figure 2c,d). The C1 ketone group in compounds **4** and **5** was proposed as the likely reduction site. Such reduction would then result in angucycline derivatives that were previously shown to be unstable and easily oxidized in the presence of light.[30] Accordingly, the enzymatic reactions were performed in the dark. NMR analysis of the reaction product of **4** resulted in the identification of **7** as the previously reported angucycline 1-deoxy-1-hydroxy-8-*O*-methylrabelomycin,[31] which was also isolated earlier from *Streptomyces* sp. QL37[14] (Table S4, Data S2). Conversely, NMR analysis of the reaction product of **5** resulted in the identification of **8** as the previously reported angucycline SM 196 B[30] (Table S4, Data S3). The results confirmed that LugOII catalyzes a C1 reduction, which is a reaction that has not previously been reported for this kind of enzyme.

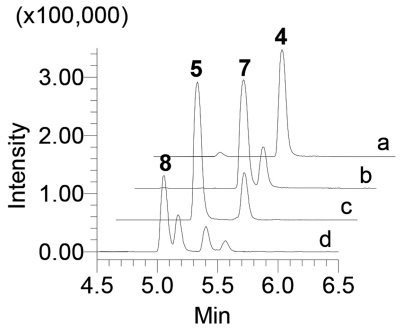

Figure 2. Extracted-ion chromatogram (XIC) overlay of the ion peaks of all the related compounds from the *in vitro* reactions. Enzymatic reactions: (a) **4**; (b) **4** + LugOII; (c) **5**; (d) **5** + LugOII. The experiments were independently repeated three times with similar results.

X-ray Crystallography Reveals Dual Functionality of LugOII. To understand the biochemistry of the C1 reduction in high mechanical detail, we analyzed the structure of the purified enzyme with and without substrates by X-ray crystallography. For this, LugOII was overexpressed and purified to homogeneity. Hexagonal and monoclinic crystals allowed one to determine the structures of *apo*-LugOII (PDB ID Code 6YQ6) and LugOII with NADPH (PDB ID Code 6YPZ) to 2.0 and 1.1 Å resolution, respectively. We also resolved the crystal structures with the substrates **4** (1.5 Å, PDB ID Code 6YQ3) and **5** (1.1 Å, PDB ID Code 6YQ0) to obtain mechanistic insights into the enzymatic reaction in the active site of the enzyme. Data acquisition and refinement statistics are summarized in Table S3. Figure 3A presents a stereoview of the NADPH-liganded structure, which adopts the canonical Rossman fold, as seen in other homologous enzymes. This is similar to, e.g., ActKR[16] and UrdMred[18] from a type II polyketide synthase, TylKR[19] from a type I polyketide synthase, and FabG[32] from a type II fatty acid synthase. The same dimeric configuration is found in each asymmetric unit of all four crystals. A sequence and structural homologue search[33] indicated that LugOII belongs to the SDR and FabG superfamily (Pfam 13561), characterized by a highly similar α/β fold but with diverse functions.[34]

DALI[33] superimposition of *apo*-LugOII with the NADPH-liganded LugOII and with two substrates liganded to LugOII resulted in a root-mean-square deviation of Cα positions (RMSD) of around 1.1 Å (Figure 3B), while superimposition of all ligand-bound structures retained an RMSD of 0.2−0.5 Å (Figure 3C). The structure of NADPH-liganded LugOII differs significantly from that of the *apo*-enzyme (Figure 3). In the latter, a subdomain "lid" formed by the helices α6 and α7 and the nearby loop region has closed down on the α/β-subdomain of the enzyme. Flipping of α6 drives the rotation of α7 by

https://dx.doi.org/10.1021/acschembio.0c00564
ACS Chem. Biol. 2020, 15, 2529−2538

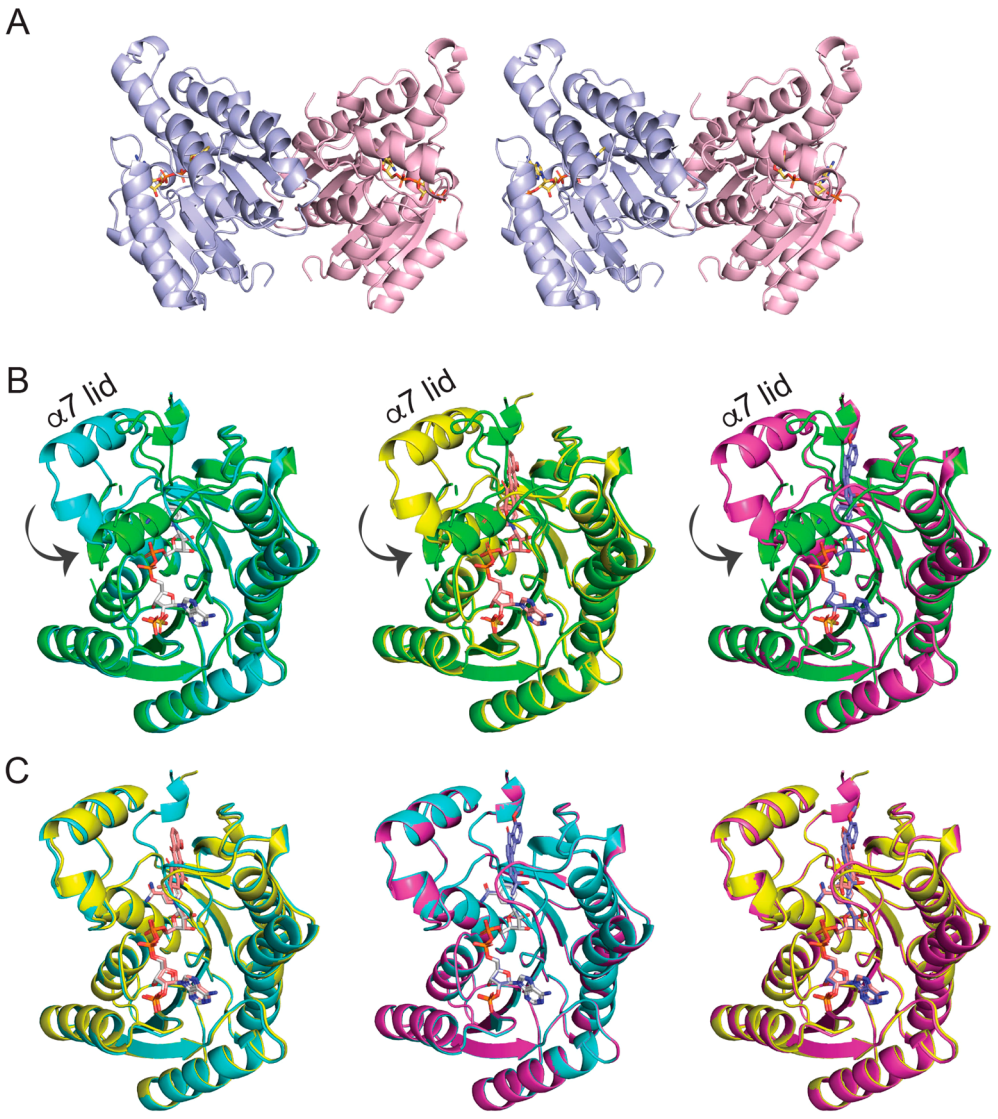

Figure 3. Dimeric arrangement of LugOII structures and observed conformational changes. (A) Stereoscopic view of NADPH-bound LugOII in dimeric form. (B) Unliganded LugOII (green), LugOII/NADPH (cyan), LugOII/NADPH/**4** (yellow), and LugOII/NADPH/**5** (magenta) structures are superimposed. α6, α7, and the loop region between them serve as a lid, which turn around 180° and then rotate 90° toward the binding site of **5**. (C) Alignment of LugOII/NADPH (cyan), LugOII/NADPH/**4** (yellow), and LugOII/NADPH/**5** (magenta) structures. NADPH, **4**, and **5** are displayed in sticks.

~90° toward the substrate binding site (Figure 3B), thereby closing the active site pocket. This switches to an open conformation upon binding of a cofactor and/or ligand and stays open until the end of the reaction, as evidenced from the alignment of all the structures in Figure 3. On the basis of the sequence alignment (Figure S2) and on previous studies,[35] the α6–α7 motif is the least conserved region. Small conformational changes in this motif have been reported in many homologous enzymes, such as ActKR,[16] SimC7,[36] and FabG.[32] However, the large conformational change we report for LugOII is rare in the KRs involved in natural product biosynthesis, suggesting significant differences and a potential benefit of shielding the active site residues in the absence of NADPH.

As described above, our metabolomic data suggested that compounds **4** and **5** are substrates for LugOII. Co-crystallization of LugOII with **4** and **5** produced clear densities for both ligands, except for the partially missing densities for the A-ring of **4**. Each ligand was bound in a deep crevice (Figure 4A,B), which positions the substrate for catalysis mainly through hydrophobic interactions. As can be seen in Figure 4C,D, the NADPH nicotinamide, together with either **4** or **5**, is perfectly aligned with the strictly conserved catalytic triad Ser149–Tyr162–Lys166 that is seen in most natural product ketoreductases (KRs).[35] With a Cα RMSD of 0.1–0.5 Å, two substrate-bound structures showed high similarity, indicating no significant conformational change during catalysis. Compound **4** was bound in a similar way compared to rabelomycin and 11-deoxylandomycinone that are found in the structure of LanV (PDB ID 4KWI) and UrdMred (PDB ID 4OSP) (Figures 4C and 6A,B), indicating a similar catalytic mechanism of LugOII in terms of the C6 reduction. However, compound **5** was oriented approximately 180° compared to compound **4**, thus positioning the C1 ketone group of **5** toward the catalytic triad, making it a perfect model for the detailed analysis of the mechanism of C1 reduction (Figure 4E,F).

https://dx.doi.org/10.1021/acschembio.0c00564
ACS Chem. Biol. 2020, 15, 2529–2538

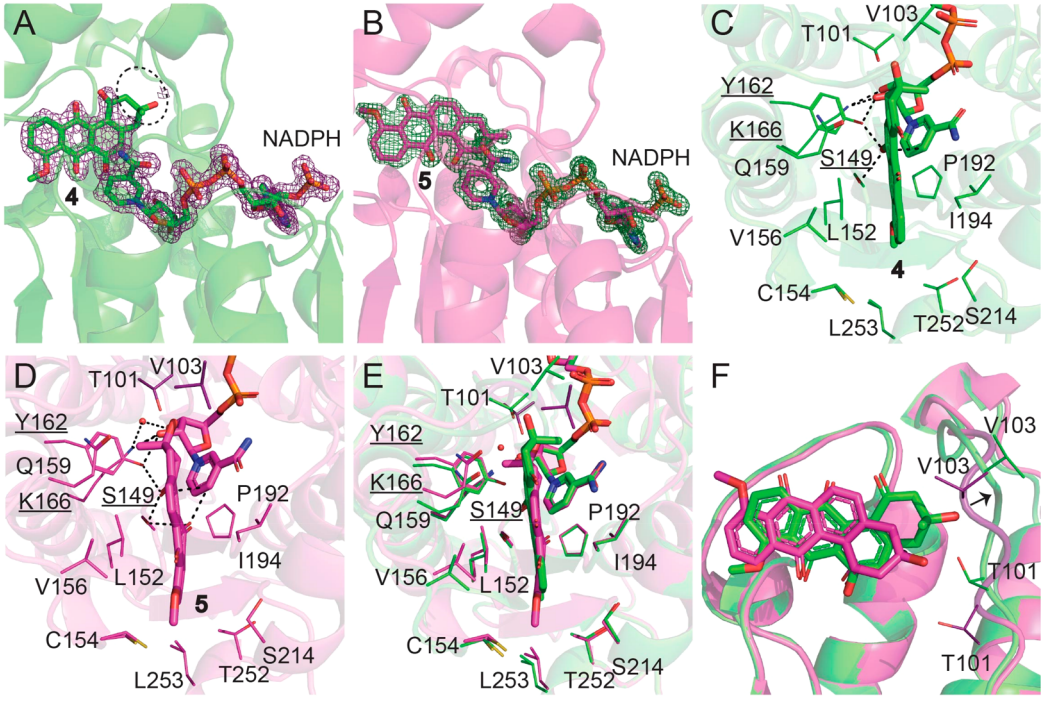

Figure 4. Active site of LugOII. (A, B) $2F_o - F_c$ omit maps contoured at the 1σ level corresponding to ligands **4** and **5** and cofactor NADPH. The missing density for **4** is highlighted with a black circle. (C, D) Key residues that surround the binding site of **4** and **5**. Catalytic residues Ser149, Tyr162, and Lys166 are underlined, and their distances (within 3.2 Å) to the ligand and cofactor are dashed. (E, F) Superposition of the two substrates **4** and **5** bounded to LugOII. (E) Top view of the active pocket. (F) Side view of the two aligned substrate structures. Major differences are found in the orientations of the two substrates and the movement of the $\alpha4-\beta4$ loop that are close to the A-rings of the two substrates. See also Figure S6.

As shown in Figure 5, the C1 ketone of **5** is hydrogen bonded to both Ser149 and Tyr162 that constitute the oxyanion hole. Attacking by the *pro*-4(*S*) proton from the NADPH carbonyl from "above" yields a C1 alkoxide that is stabilized by the hydrogen bonds of Ser149 and Tyr162. The conserved Tyr162 residue serves as central acid−base catalyst that donates a proton to the substrate, while the adjacent K166 residue lowers the pK_a of the hydroxyl group of Tyr162, thus contributing directly to the proton relay system. The hydroxyl group of S149 stabilizes and polarizes the carbonyl group of the substrate. The relative configuration of the two hydroxyl groups at C1 and C3 was assigned as *trans* on the basis of the electron densities and the position of **5** in the active sites of LugOII (Figure 5). As the absolute configuration at C3 in compound **5** was confirmed to be *R* by total synthesis,[37] an *S*-configuration could thus be assigned to C1. The reaction mechanism of **4** to **7** could also be deduced similarly. The catalytic mechanism of C1 reduction resembles that of C6 reduction that occurs in the other homologous enzymes LanV and UrdMred[18] but also differs in many ways, which are discussed later.

Key Features in the Active Site of LugOII. Our enzymatic and structural analyses highlight LugOII as a promiscuous enzyme that catalyzes C1 reduction of both **4** and **5**. We therefore wondered how both reactions could be catalyzed by a single active site. On inspection of the two substrate−liganded structures, movement of the $\alpha4-\beta4$ loop was observed not only in LugOII complexed with **4** and **5** but also in different chains of one specific structure (Figure S6). As shown in Figure 4F, the A-ring of **5** resides much more downward than that of **4** to cover the A-ring, while the $\alpha4-\beta4$ loop also adopts a more closed position. That is, the A-ring of **4** cannot fit into the "normal" pocket of **5**. The same effect can also be seen in LanV and UrdM[18] complex structures, where the A-ring of rabelomycin and 11-deoxylandomycinone collapse in the "normal" pocket (Figure 6D). This movement can be attributed to a steric effect, in other words, with the movement as the driving force for substrate rotation. Notably, the loop region in LugOII is extended by two residues (Val103 and Asp104) as compared to LanV and UrdM,[18] and we therefore hypothesize that this makes LugOII more dynamic.

Residues Cys154 and Ser214 at the end of the active site replace residues Val152 and Leu212 in LanV (PDB ID 4KWI) and Phe152 and Tyr212 in UrdMred (PDB ID 4OSP), respectively. The bulkier residues that are found in LanV[17] and UrdMred[18] structures decrease the volume of the active site, which may act as "gatekeepers" that affect the substrate rotation. Cys154 was found to adopt different confirmations in both compound **4** and **5** complexed structures (Figure 4C,D). Superimposition of **5** into the active cavity of UrdMred shows a clash between the 8-*O*-methyl group of **5** and the phenyl moiety of Phe152 (Figure 6C). Similarly, Thr101 in the $\alpha4-\beta4$ loop region of LugOII is replaced by a methionine in its orthologues. Finally, the 2-methyl group of **5** and the 4-thio group of M101 are at only a 1.0−1.7 Å distance, which should sterically affect substrate rotation (Figure 6C).

Site-Directed Mutagenesis of Active Site Residues. To validate the structural data, we probed the positions that contain the $\alpha4-\beta4$ loop region (Val103, Asp104) and the active site residues (Cys154, Ser214, and Thr101). Val156, Gln159, and Ile194 were also chosen, as they were predicted to play important roles in LanV, UrdMred, and other KRs. To investigate their roles in the dual function of LugOII, we created site-directed mutants and expressed the protein

https://dx.doi.org/10.1021/acschembio.0c00564
ACS Chem. Biol. 2020, 15, 2529−2538

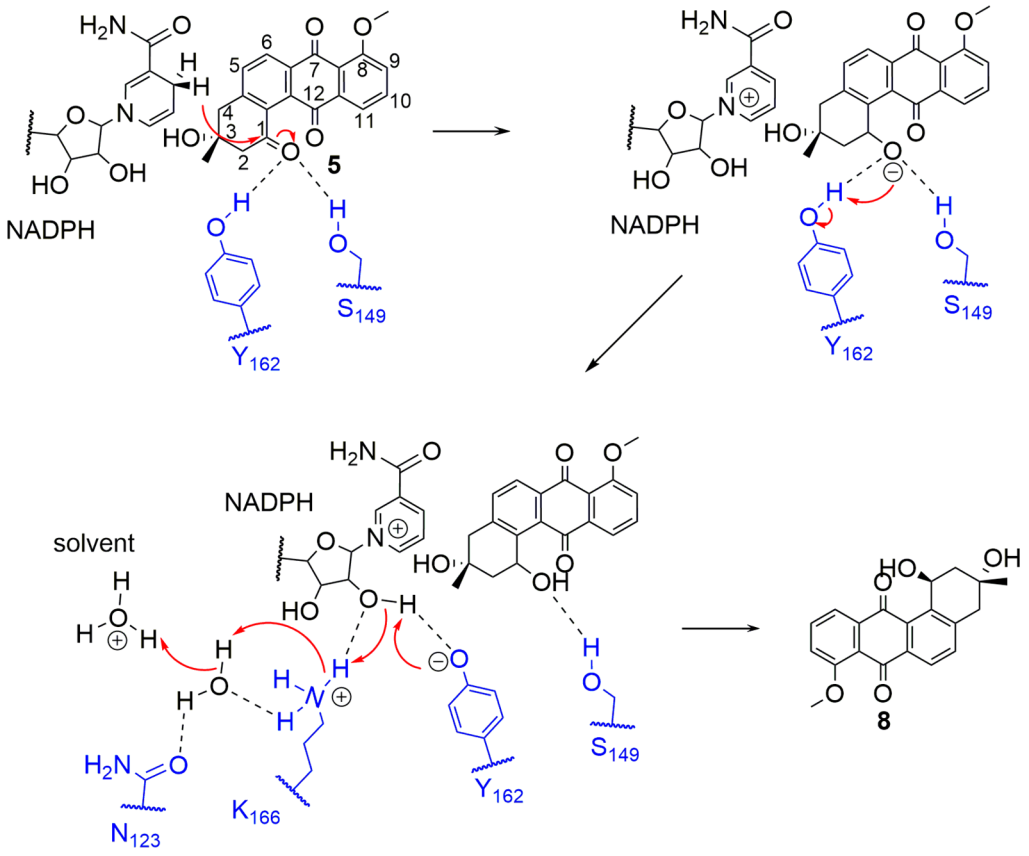

Figure 5. Postulated catalytic mechanism for the LugOII-catalyzed C1 reduction and proton relay. The reaction is initiated by proton transfer from the hydroxyl group of Tyr162 to the carbonyl group of **5**, followed by a hydride transfer to the C1 position of **5**. The catalytic triad (Lys166, Tyr162, and Ser149) and N123 are highlighted in blue.

variants for *in vitro* enzymatic assays. While residues Val103 and Asp104 were deleted, Cys154, Ser214, and Thr101 were mutated to the bulkier residues Phe, Tyr, and Met, respectively. Furthermore, Val156 and Gln159 were substituted by alanine, and Ile194 was substituted by a serine residue.

Enzymatic activity was measured through the relative NADPH consumption rate by UV absorption scanning at 340 nm, using **5** as the precursor in the reaction (Figure 7). The V156A, C154F, ΔV103, and S214Y mutants showed similar NADPH consumption rates compared to the wild-type enzyme (Figure 7), indicating that these residues did not play a role in LugOII activity. In the mutant lacking Val103 and Asp104 in the $\alpha4-\beta4$ loop region, the conversion rate was slightly reduced (Figure 7). Conversely, the conversion rate of **5** was greatly reduced in mutant Q159A. The glutamine residue in the equivalent site of LanV[17] and UrdM[18] interacts with the ligand, while in LugOII, it acts as an anchor point for the correct positioning of the $\alpha4-\beta4$ loop (Figure S7). A similar effect was seen in the T101 M mutant, where the conversion rate was dramatically decreased. As T101 interacts with the 3-hydroxyl group of compounds **4** and **5** (Figures S5 and S7), the mutation to methionine has less effect on ligand **4** but clashes with ligand **5** (Figure 6A,C). Clearly, the substitution of Ile194 by a serine has a strong influence on the catalytic activity of the C1 reduction (Figure 6A,C), which supports the essential role of the equivalent isoleucine residue in LanV[17] and UrdM,[18] in terms of substrate specificity and stereoselectivity. These data highlight the key role of Thr101, Gln159, and Ile194 plus the motion of the $\alpha4-\beta4$ loop in the dual functionality of LugOII, which is consistent with the analysis of ligand **4** and **5** bounded structures.

In summary, combined mutational, enzymatic, and structural analysis shows that besides the C6 ketoreduction, LugOII also possesses an unprecedented C1 ketoreduction, generating the two angucycline derivatives **7** and **8**. The *apo*- and complexed structures of LugOII shed light on several novel features near the active center. A significant conformational change occurs prior to catalysis, which is mainly achieved by flipping of the $\alpha6-\alpha7$ motif. Additionally, mutagenesis showed that residue Thr101 stabilizes the orientation of the substrate via a hydrogen bond, leaving sufficient space to allow the entry of different substrates (compounds **4** and **5**) for the catalysis of C1 reduction. The loop region that harbors Thr101 is also of importance to the catalytic activity of LugOII, as the activity was slightly decreased in mutants lacking Val103 and Asp104. Furthermore, the mutation of Gln159, which mediates the localization of the $\alpha4-\beta4$ loop, led to a significant decrease in the C1 reduction activity. It was also found that Ile194 contributes largely to the dual functionality of LugOII, which is likely mediated via a hydrophobic interaction with the ligands. Overall, our results provide new insights into the structure and catalytic mechanism of a novel promiscuous reductase in angucycline biosynthesis. Since angucyclines are one of the most diverse and important families of polyketides, LugOII is a promising candidate for its application in the synthesis of novel regio- and stereochemically diverse polyketide antibiotics.

https://dx.doi.org/10.1021/acschembio.0c00564
ACS Chem. Biol. 2020, 15, 2529−2538

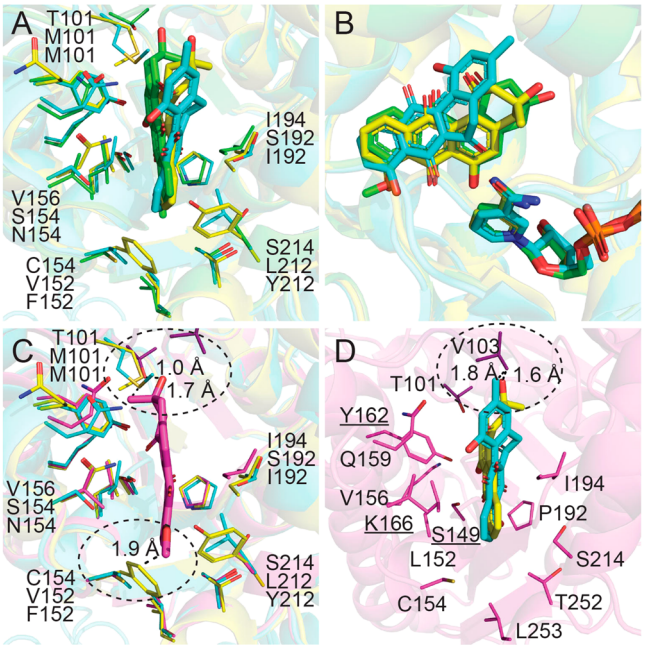

Figure 6. Superposition of LugOII (green for **4** and magenta for **5**), LanV (cyan, PDB entry, 4KWI), and UrdMred (yellow, PDB entry, 4OSP) reveals major differences in the active sites. (A, B) LugOII/**4**, LanV, and UrdMred structures are aligned. (C) **5** is superposed in the active pocket of LanV and UrdMred. Clashes were seen in two regions (highlighted by circles). One region is the extra loop between α4 and β4 in which Thr101 of LugOII is replaced by Met101 of LanV and UrdMred. The other region represents residues Cys154 and Ser214 that are near the D-ring binding site. They were substituted by Val152 and Tyr212 in LanV and Phe152 and Leu212 in UrdMred, respectively. (D) 11-Deoxylandomycinone of LanV and rabelomycin of UrdMred are superposed in the LugOII active pocket, where Val103 of LugOII clashes with the 3-methyl and 3-hydroxyl groups of the A-ring, respectively.

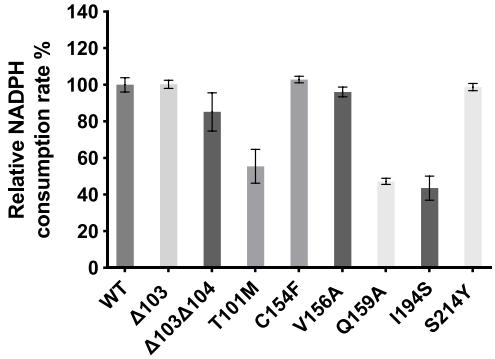

Figure 7. Enzymatic activity of LugOII variants. The columns represent the relative activity of LugOII variants compared to that of the wild-type enzyme, based on the consumption rate of NADPH by measuring the UV absorbance at 340 nm. Reactions were carried out using compound **5** as the substrate. The experiments were independently repeated three times with similar results.

METHODS

Strains, Mutants, and Genetic Complementation. *Streptomyces* sp. QL37 was isolated from the Qinling mountains in China.[38] Strains were grown on MM or R5 agar plates.[39] For details on strains and culturing conditions, see the Supplemental Methods. An in-frame deletion mutant of *lugOII* was obtained via homologous recombination.[40] For generation of the knockout construct, the up- and downstream (~1.5 kb) regions of *lugOII* were amplified with the primer pairs lugOII_LF_Fw/lugOII_LF_Rv and lugOII_RF_Fw/lugOII_RF_Rv, respectively, from genomic DNA of *Streptomyces* sp. QL37. The PCR products were cloned into the conjugative vector pWHM3-*oriT*.[41] The apramycin resistance cassette (*aac(3)IV*) flanked with *loxP* sites was cloned between the upstream and downstream region of *lugOII*. To obtain *lugOII* null mutants, the plasmids were introduced into *Streptomyces* sp. QL37 via conjugative transfer from *E. coli* ET12567/pUZ8002[39] and lawns of the transformants replicated nonselectively to allow double recombination. In this way, a mutant was obtained whereby the chromosomal *lugOII* was replaced by the apramycin resistance cassette. Cre recombinase was expressed via introduction of plasmid pUWL-Cre[42] to remove the apramycin cassette, resulting in an in-frame deletion mutant lacking the +12/+1947 region relative to the translational start site of *lugOII*. The mutant was verified by PCR and DNA sequencing.

For genetic complementation, *lugOII* was amplified using primers lugOII_OE_Fw/lugOII_OE_Rv. The insert was placed under the control of an *ermE* promoter. The integrity of the construct was verified by sequencing. The plasmid was conjugated to *Streptomyces* sp. QL37 and *Streptomyces* sp. QL37 (Δ*lugOII*) using *E. coli* ET12567/pUZ8002[39] as the donor strain. Primers are listed in Table S2.

Protein Crystallization, Data Collection, and Structure Solution. To obtain protein for crystallization and enzymatic experiments, LugOII was cloned into pET-28a (+) vector (Novagen). LugOII active site mutants were generated by whole plasmid synthesis (WHOPS) based on the instructions of Quik Change* Site-Directed Mutagenesis (Stratagene). All constructs were sequenced before use. The plasmid expressing LugOII was transformed into *E. coli* BL21 (DE3) pLysS Star (Invitrogen), and the N-terminal His_6-tagged protein was expressed and purified as described.[43] All crystallization experiments of LugOII were conducted with N-terminal His_6-tag (21.8 mg mL^{-1}) by sitting-drop vapor diffusion at 18 °C. Monoclinic apo-LugOII crystals (apo form) were obtained in 0.3 M NaCl, 0.1 M Na cacodylate, pH 6.5, 1.5 M $(NH_4)_2SO_4$. For cocrystallization, NADPH was added to LugOII to a final concentration of 1 mM and $^1/_{10}$ vol of a saturated solution of either **4** or **5**. Brown color crystals of both complex forms grew from the condition of 16−22% (w/v) PEG3350, 0−0.1 M Na malonate, 0.1 M BIS-Tris prop, pH 6.5. Crystals were cryoprotected by supplementing the crystallization solution with 20% (v/v) PEG400 or ethylene glycol (EG).

Diffraction data were collected at the Swiss Light Source at beamline X06DA (PXIII) and theNational Synchrotron Radiation Research Center, Taiwan, respectively. The data were further indexed, integrated using XDS,[44] and scaled and merged using AIMLESS[45] from the CCP4 package.[46] Phases of all the LugOII structures were solved by molecular replacement with MOLREP,[47] using UrdMred[18] (PDB entry 4OSP) as the template. The models of apo and complex structures were completed by several iterations of manual building in COOT[48] and restrained refinement in REFMAC5[49] using isotropic B factors. The PRODRG server[50] was used to generate the coordinate files for the ligand of the binary complex. Structures were finalized by several rounds of TLS and restrained refinement in REFMAC5 and validated using the wwPDB validation service.[51] Residues were in the most favored regions of the Ramachandran plot[52] as determined by PROCHECK.[53] The resultant data collection, processing, and refinement statistics are summarized in Table S3.

Enzymatic Reactions. For the enzymatic reaction with **4** or **5**, the reaction mixture (100 μL) containing LugOII buffer (25 mM Tris, 155 mM NaCl, 5% (w/v) glycerol, 20 mM β-mercaptoethanol, pH 7.5), compound **4** or **5** (~100 μM), LugOII (2 μM), and NADPH (1 mM) was incubated at 30 °C for 30 min. A control reaction was performed with heat-inactivated LugOII. The reactions were acidified by HCl to pH 3−4 and extracted with ethyl acetate (3 × 100 μL). Reaction products were checked by LC-MS and NMR as described,[14,54] followed by comparison with the literature. For details, see the Supplemental Methods.

https://dx.doi.org/10.1021/acschembio.0c00564
ACS Chem. Biol. 2020, 15, 2529−2538

Metabolic Analysis. HPLC purifications were performed on a Waters preparative HPLC system equipped with a photodiode array detector (PDA). The absorption was monitored at 220, 290, and 350 nm. LC-MS analysis was performed on a Shimadzu LC-MS 9030 system composed of a UPLC with an attached PDA, coupled to a QTOF HRMS, which uses ESI as an ionization source. NMR spectra were acquired on a Bruker AVIII-600 NMR spectrometer (Bruker BioSpin GmbH). For details on metabolite extraction and analysis, see the Supplemental Methods.

■ ASSOCIATED CONTENT

Supporting Information

The Supporting Information is available free of charge at https://pubs.acs.org/doi/10.1021/acschembio.0c00564.

Supplemental methods for strains and culturing conditions, metabolite isolation and characterization, and LC-MS/MS methodology; graphical representation of the *lug* gene cluster; SDS-PAGE analysis; multi-sequence alignment of LugOII; unrooted maximum likelihood tree of the KRs that are related to LugOII; interactions between the ligands and the key residues of LugOII structure; alignment of the different chains from LugOII complex structures; interaction network of Q159 in LugOII complex structures; supplemental data and spectra; bacterial strains used in this study; primers; X-ray data collection, processing, and refinement; ^{1}H and ^{13}C NMR data (PDF)

Accession Codes

The atomic coordinates of the LugOII structures have been deposited in the Protein Data Bank (ID: 6YQ6, 6YPZ, 6YQ3, and 6YQ0).

■ AUTHOR INFORMATION

Corresponding Author

Gilles P. van Wezel − *Molecular Biotechnology, Leiden University, 2300RA Leiden, The Netherlands;* orcid.org/0000-0003-0341-1561; Email: g.wezel@biology.leidenuniv.nl

Authors

Xiansha Xiao − *Molecular Biotechnology, Leiden University, 2300RA Leiden, The Netherlands*

Somayah S. Elsayed − *Molecular Biotechnology, Leiden University, 2300RA Leiden, The Netherlands;* orcid.org/0000-0003-3837-6137

Changsheng Wu − *State Key Laboratory of Microbial Technology, Institute of Microbial Technology, Shandong University, Qingdao, Shandong 266237, P. R. China*

Helga U. van der Heul − *Molecular Biotechnology, Leiden University, 2300RA Leiden, The Netherlands*

Mikko Metsä-Ketelä − *Department of Biochemistry and Food Chemistry, University of Turku, FIN-20014 Turku, Finland;* orcid.org/0000-0003-3176-2908

Chao Du − *Molecular Biotechnology, Leiden University, 2300RA Leiden, The Netherlands*

Andrea E. Prota − *Laboratory of Biomolecular Research, Division of Biology and Chemistry, Paul Scherrer Institut, CH-5232 Villigen, Switzerland*

Chun-Chi Chen − *State Key Laboratory of Biocatalysis and Enzyme Engineering, School of Life Sciences, Hubei University, Wuhan, Hubei 43420, P. R. China;* orcid.org/0000-0002-7459-5591

Weidong Liu − *State Key Laboratory of Biocatalysis and Enzyme Engineering, School of Life Sciences, Hubei University, Wuhan, Hubei 43420, P. R. China*

Rey-Ting Guo − *State Key Laboratory of Biocatalysis and Enzyme Engineering, School of Life Sciences, Hubei University, Wuhan, Hubei 43420, P. R. China;* orcid.org/0000-0002-2779-7115

Jan Pieter Abrahams − *Molecular Biotechnology, Leiden University, 2300RA Leiden, The Netherlands; Bio-nano diffraction Biozentrum, Paul Scherrer Institut, CH-5232 Villigen, Switzerland; Biozentrum, University of Basel, CH-4058 Basel, Switzerland*

Complete contact information is available at: https://pubs.acs.org/10.1021/acschembio.0c00564

Notes

The authors declare no competing financial interest.

■ ACKNOWLEDGMENTS

We thank E. de Waal for technical assistance. We gratefully acknowledge the Swiss Light Source, Villigen PSI, Switzerland, and National Synchrotron Radiation Research Center, Taiwan. This work was supported by a grant from the Chinese Scholarship Council (CSC) to X.X. and by grant 16439 from The Netherlands Organization for Scientific Research (NWO) to G.P.W.

■ REFERENCES

(1) Kharel, M. K., Pahari, P., Shepherd, M. D., Tibrewal, N., Nybo, S. E., Shaaban, K. A., and Rohr, J. (2012) Angucyclines: biosynthesis, mode-of-action, new natural products, and synthesis. *Nat. Prod. Rep. 29*, 264−325.

(2) Ostash, B., Korynevska, A., Stoika, R., and Fedorenko, V. (2009) Chemistry and biology of landomycins, an expanding family of polyketide natural products. *Mini-Rev. Med. Chem. 9*, 1040−1051.

(3) Drautz, H., Zahner, H., Rohr, J., and Zeeck, A. (1986) Metabolic products of microorganisms. 234. Urdamycins, new angucycline antibiotics from *Streptomyces fradiae*. I. Isolation, characterization and biological properties. *J. Antibiot. 39*, 1657−1669.

(4) Yang, K., Han, L., and Vining, L. C. (1995) Regulation of jadomycin B production in *Streptomyces venezuelae* ISP5230: involvement of a repressor gene, *jadR2*. *J. Bacteriol. 177*, 6111−6117.

(5) Takahashi, K., Yoshida, M., Tomita, F., and Shirahata, K. (1981) Gilvocarcins, new antitumor antibiotics. 2. Structural elucidation. *J. Antibiot. 34*, 271−275.

(6) Rohr, J., and Thiericke, R. (1992) Angucycline group antibiotics. *Nat. Prod. Rep. 9*, 103−137.

(7) Hertweck, C., Luzhetskyy, A., Rebets, Y., and Bechthold, A. (2007) Type II polyketide synthases: gaining a deeper insight into enzymatic teamwork. *Nat. Prod. Rep. 24*, 162−190.

(8) Barka, E. A., Vatsa, P., Sanchez, L., Gavaut-Vaillant, N., Jacquard, C., Meier-Kolthoff, J., Klenk, H. P., Clément, C., Oudouch, Y., and van Wezel, G. P. (2016) Taxonomy, physiology, and natural products of the *Actinobacteria*. *Microbiol. Mol. Biol. Rev. 80*, 1−43.

(9) Bérdy, J. (2005) Bioactive microbial metabolites. *J. Antibiot. 58*, 1−26.

(10) Kolter, R., and van Wezel, G. P. (2016) Goodbye to brute force in antibiotic discovery? *Nat. Microbiol 1*, 15020.

(11) Nett, M., Ikeda, H., and Moore, B. S. (2009) Genomic basis for natural product biosynthetic diversity in the actinomycetes. *Nat. Prod. Rep. 26*, 1362−1384.

(12) Rutledge, P. J., and Challis, G. L. (2015) Discovery of microbial natural products by activation of silent biosynthetic gene clusters. *Nat. Rev. Microbiol. 13*, 509−523.

(13) van Bergeijk, D. A., Terlouw, B. R., Medema, M. H., and van Wezel, G. P. (2020) Ecology and genomics of Actinobacteria: new

concepts for natural product discovery. *Nat. Rev. Microbiol.*, DOI: 10.1038/s41579-020-0379-y.
(14) Wu, C., van der Heul, H. U., Melnik, A. V., Lubben, J., Dorrestein, P. C., Minnaard, A. J., Choi, Y. H., and van Wezel, G. P. (2019) Lugdunomycin, an angucycline-derived molecule with unprecedented chemical architecture. *Angew. Chem., Int. Ed. 58*, 2809−2814.
(15) Uiterweerd, M. T., Nuñez Santiago, I., van der Heul, H. U., van Wezel, G. P., and Minnaard, A. J. (2020) Iso-maleimycin, a constitutional isomer of maleimycin, from *Streptomyces* sp. QL37. *Eur. J. Org. Chem.*, 5145−5152.
(16) Javidpour, P., Bruegger, J., Srithahan, S., Korman, T. P., Crump, M. P., Crosby, J., Burkart, M. D., and Tsai, S. C. (2013) The determinants of activity and specificity in actinorhodin type II polyketide ketoreductase. *Chem. Biol. 20*, 1225−1234.
(17) Paananen, P., Patrikainen, P., Kallio, P., Mantsala, P., Niemi, J., Niiranen, L., and Metsä-Ketelä, M. (2013) Structural and functional analysis of angucycline C-6 ketoreductase LanV involved in landomycin biosynthesis. *Biochemistry 52*, 5304−5314.
(18) Patrikainen, P., Niiranen, L., Thapa, K., Paananen, P., Tahtinen, P., Mantsala, P., Niemi, J., and Metsä-Ketelä, M. (2014) Structure-based engineering of angucyclinone 6-ketoreductases. *Chem. Biol. 21*, 1381−1391.
(19) Keatinge-Clay, A. T. (2007) A tylosin ketoreductase reveals how chirality is determined in polyketides. *Chem. Biol. 14*, 898−908.
(20) Kallio, P., Patrikainen, P., Suomela, J.-P., Mäntsälä, P., Metsä-Ketelä, M., and Niemi, J. (2011) Flavoprotein hydroxylase PgaE catalyzes two consecutive oxygen-dependent tailoring reactions in angucycline biosynthesis. *Biochemistry 50*, 5535−5543.
(21) Patrikainen, P., Kallio, P., Fan, K. Q., Klika, K. D., Shaaban, K. A., Mantsala, P., Rohr, J., Yang, K. Q., Niemi, J., and Metsä-Ketelä, M. (2012) Tailoring enzymes involved in the biosynthesis of angucyclines contain latent context-dependent catalytic activities. *Chem. Biol. 19*, 647−655.
(22) Zhu, L., Ostash, B., Rix, U., Nur, E. A. M., Mayers, A., Luzhetskyy, A., Mendez, C., Salas, J. A., Bechthold, A., Fedorenko, V., and Rohr, J. (2005) Identification of the function of gene lndM2 encoding a bifunctional oxygenase-reductase involved in the biosynthesis of the antitumor antibiotic landomycin E by *Streptomyces globisporus* 1912 supports the originally assigned structure for landomycinone. *J. Org. Chem. 70*, 631−638.
(23) Jackson, D. R., Yu, X., Wang, G. J., Patel, A. B., Calveras, J., Barajas, J. F., Sasaki, E., Metsä-Ketelä, M., Liu, H. W., Rohr, J., and Tsai, S. C. (2016) Insights into complex oxidation during BE-7585A biosynthesis: structural determination and analysis of the polyketide monooxygenase BexE. *ACS Chem. Biol. 11*, 1137−1147.
(24) Kallio, P., Liu, Z. L., Mantsala, P., Niemi, J., and Metsä-Ketelä, M. (2008) Sequential action of two flavoenzymes, PgaE and PgaM, in angucycline biosynthesis: chemoenzymatic synthesis of gaudimycin C. *Chem. Biol. 15*, 157−166.
(25) Kallio, P., Liu, Z., Mantsala, P., Niemi, J., and Metsä-Ketelä, M. (2008) A nested gene in *Streptomyces* bacteria encodes a protein involved in quaternary complex formation. *J. Mol. Biol. 375*, 1212−1221.
(26) Liu, T., Fischer, C., Beninga, C., and Rohr, J. (2004) Oxidative rearrangement processes in the biosynthesis of gilvocarcin V. *J. Am. Chem. Soc. 126*, 12262−12263.
(27) Yang, C. F., Huang, C. S., Zhang, W. J., Zhu, Y. G., and Zhang, C. S. (2015) Heterologous expression of fluostatin gene cluster leads to a bioactive heterodimer. *Org. Lett. 17*, 5324−5327.
(28) Metsä-Ketelä, M., Palmu, K., Kunnari, T., Ylihonko, K., and Mantsala, P. (2003) Engineering anthracycline biosynthesis toward angucyclines. *Antimicrob. Agents Chemother. 47*, 2063−2063.
(29) Kulowski, K., Wendt-Pienkowski, E., Han, L., Yang, K. Q., Vining, L. C., and Hutchinson, C. R. (1999) Functional characterization of the jadI gene as a cyclase forming angucyclinones. *J. Am. Chem. Soc. 121*, 1786−1794.
(30) Grabley, S., Hammann, P., Hutter, K., Kluge, H., Thiericke, R., Wink, J., and Zeeck, A. (1991) Secondary metabolites by chemical-screening. Part 19. Sm-196-a and Sm-196-B, novel biologically-active angucyclinones from *Streptomyces* Sp. *J. Antibiot. 44*, 670−673.
(31) Fotso, S., Mahmud, T., Zabriskie, T. M., Santosa, D. A., and Proteau, P. J. (2008) Rearranged and unrearranged angucyclinones from Indonesian *Streptomyces* spp. *J. Antibiot. 61*, 449−456.
(32) Price, A. C., Zhang, Y. M., Rock, C. O., and White, S. W. (2004) Cofactor-induced conformational rearrangements establish a catalytically competent active site and a proton relay conduit in FabG. *Structure 12*, 417−428.
(33) Holm, L. (2019) Benchmarking fold detection by DaliLite v.5. *Bioinformatics 35*, 5326−5327.
(34) Filling, C., Berndt, K. D., Benach, J., Knapp, S., Prozorovski, T., Nordling, E., Ladenstein, R., Jornvall, H., and Oppermann, U. (2002) Critical residues for structure and catalysis in short-chain dehydrogenases/reductases. *J. Biol. Chem. 277*, 25677−25684.
(35) Oppermann, U., Filling, C., Hult, M., Shafqat, N., Wu, X., Lindh, M., Shafqat, J., Nordling, E., Kallberg, Y., Persson, B., and Jornvall, H. (2003) Short-chain dehydrogenases/reductases (SDR): the 2002 update. *Chem.-Biol. Interact. 143−144*, 247−253.
(36) Schafer, M., Stevenson, C. E. M., Wilkinson, B., Lawson, D. M., and Buttner, M. J. (2016) Substrate-assisted catalysis in polyketide reduction proceeds via a phenolate intermediate. *Cell Chem. Biol. 23*, 1091−1097.
(37) Kesenheimer, C., and Groth, U. (2006) Total synthesis of (−)-8-O-methyltetrangomycin (MM 47755). *Org. Lett. 8*, 2507−2510.
(38) Zhu, H., Swierstra, J., Wu, C., Girard, G., Choi, Y. H., van Wamel, W., Sandiford, S. K., and van Wezel, G. P. (2014) Eliciting antibiotics active against the ESKAPE pathogens in a collection of actinomycetes isolated from mountain soils. *Microbiology 160*, 1714−1725.
(39) Kieser, T., Bibb, M. J., Buttner, M. J., Chater, K. F., and Hopwood, D. A. (2000) *Practical Streptomyces genetics*, John Innes Foundation, Norwich, U.K.
(40) Swiatek, M. A., Tenconi, E., Rigali, S., and van Wezel, G. P. (2012) Functional analysis of the N-acetylglucosamine metabolic genes of *Streptomyces coelicolor* and role in the control of development and antibiotic production. *J. Bacteriol. 194*, 1136−1144.
(41) Vara, J., Lewandowska-Skarbek, M., Wang, Y. G., Donadio, S., and Hutchinson, C. R. (1989) Cloning of genes governing the deoxysugar portion of the erythromycin biosynthesis pathway in *Saccharopolyspora erythraea* (*Streptomyces erythreus*). *J. Bacteriol. 171*, 5872−5881.
(42) Fedoryshyn, M., Welle, E., Bechthold, A., and Luzhetskyy, A. (2008) Functional expression of the Cre recombinase in actinomycetes. *Appl. Microbiol. Biotechnol. 78*, 1065−1070.
(43) Mahr, K., van Wezel, G. P., Svensson, C., Krengel, U., Bibb, M. J., and Titgemeyer, F. (2000) Glucose kinase of *Streptomyces coelicolor* A3(2): large-scale purification and biochemical analysis. *Antonie van Leeuwenhoek 78*, 253−261.
(44) Kabsch, W. (2010) Xds. *Acta Crystallogr., Sect. D: Biol. Crystallogr. 66*, 125−132.
(45) Evans, P. R., and Murshudov, G. N. (2013) How good are my data and what is the resolution? *Acta Crystallogr., Sect. D: Biol. Crystallogr. 69*, 1204−1214.
(46) Collaborative Computational Project, Number 4 (1994) The ccp4 suite - programs for protein crystallography. *Acta Crystallogr., Sect. D: Biol. Crystallogr. 50*, 760−763.
(47) Vagin, A., and Teplyakov, A. (1997) MOLREP: an automated program for molecular replacement. *J. Appl. Crystallogr. 30*, 1022−1025.
(48) Emsley, P., Lohkamp, B., Scott, W. G., and Cowtan, K. (2010) Features and development of Coot. *Acta Crystallogr., Sect. D: Biol. Crystallogr. 66*, 486−501.
(49) Murshudov, G. N., Vagin, A. A., and Dodson, E. J. (1997) Refinement of macromolecular structures by the maximum-likelihood method. *Acta Crystallogr., Sect. D: Biol. Crystallogr. 53*, 240−255.

(50) Schüttelkopf, A. W., and van Aalten, D. M. (2004) PRODRG: a tool for high-throughput crystallography of protein-ligand complexes. *Acta Crystallogr., Sect. D: Biol. Crystallogr. 60*, 1355−1363.
(51) Berman, H., Henrick, K., and Nakamura, H. (2003) Announcing the worldwide Protein Data Bank. *Nat. Struct. Mol. Biol. 10*, 980−980.
(52) Ramachandran, G. N., Ramakrishnan, C., and Sasisekharan, V. (1963) Stereochemistry of polypeptide chain configurations. *J. Mol. Biol. 7*, 95−99.
(53) Laskowski, R. A., Macarthur, M. W., Moss, D. S., and Thornton, J. M. (1993) Procheck - a program to check the stereochemical quality of protein structures. *J. Appl. Crystallogr. 26*, 283−291.
(54) Wu, C., Du, C., Gubbens, J., Choi, Y. H., and van Wezel, G. P. (2015) Metabolomics-Driven Discovery of a Prenylated Isatin Antibiotic Produced by *Streptomyces* Species MBT28. *J. Nat. Prod. 78*, 2355−2363.

https://dx.doi.org/10.1021/acschembio.0c00564
ACS Chem. Biol. 2020, 15, 2529−2538